



OPEN

Hydrogel-Stabilized Droplet Bilayers for High Speed Solution Exchange

SUBJECT AREAS:

LAB-ON-A-CHIP

ASSAY SYSTEMS

BIOLOGICAL PHYSICS

BIOMEDICAL ENGINEERING

Shiv A. Acharya¹, Alexander Portman¹, Carl S. Salazar² & Jacob J. Schmidt¹¹Department of Bioengineering, University of California, Los Angeles, CA, 90095-1600, U.S.A., ²Librede Inc., Sherman Oaks, CA, 91403.Received
3 June 2013Accepted
18 October 2013Published
5 November 2013Correspondence and
requests for materials
should be addressed to
J.J.S. (schmidt@seas.
ucla.edu)

Many applications utilizing artificial lipid bilayers require the ability to exchange the bilayer's solution environment. However, because of the instability of the bilayer, the rate of solution exchange is limited, which significantly hinders the measurement rate and throughput. We have developed an artificial bilayer system that can withstand high flow speeds, up to 2.1 m/s, by supporting the bilayer with a hydrogel. We demonstrated the ability to measure during flow by measuring the conductance of gramicidin-A channels while switching between solutions of two different compositions, recording a time to measure 90% change in current of approximately 2.7 seconds at a flow rate of 0.1 m/s. We also demonstrated a potential application of this system by measuring the conductance modulation of the rat TRPM8 ion channel by an agonist and antagonist at varying concentrations, obtaining 7-point IC_{50} and EC_{50} values in approximately 7 minutes and 4-point values within 4 minutes.

Artificial lipid bilayer membranes are well established for fundamental physiological studies of ion channels^{1,2} as well as technological applications including sensing³, drug potency measurement^{4–7}, and potentially DNA sequencing⁸. In many of these applications, it is often desirable to exchange the solution surrounding the bilayer during measurement to halt ion channel incorporation for single channel studies, to introduce analyte solutions for sensing, or to measure changes in ion channel conductance with changing pharmaceutical concentrations.

Solution exchange for freestanding lipid bilayer membranes can be problematic, as the membranes are fragile, deforming or rupturing in the presence of the small transmembrane pressure differences⁹ that can result from flowing solutions^{10–12}. As a result, traditional bilayer solution perfusion is limited to low flow rates, which result in complete exchange of the surrounding solution in timescales on the order of minutes^{13–15}. Several recent papers have described microfluidic systems capable of exchanging the surrounding solution in 10–100 seconds^{10–12}. With one of these systems, we measured the potency of drugs for the TRPM8 and hERG ion channels in lipid bilayers by measuring the ion channel conductance while solutions containing increasing drug concentrations were introduced adjacent to one side of the bilayer^{4,5}. Total measurement time for 5 different concentrations was approximately 30 to 50 minutes⁵, and measurement of 8 different concentrations required approximately 80 minutes⁴ due in part to the slow rate of solution perfusion tolerable by the bilayer.

Although solid-supported lipid bilayers are robust and can withstand high solution flow rates¹⁶, they are unable to support application of constant voltages or measurement of direct currents needed for most ion channel conductance studies. These are possible with hydrogel-supported membranes; previously we have shown that hydrogel-supported membranes have increased tolerance to transmembrane pressure and greater longevity^{9,17}. Others have shown production of hydrogel bilayer “chips”^{18,19}. Most relevant to this work, bilayers formed through contact of lipid monolayers (in some contexts also called droplet interface bilayers^{20–22}) have also been shown to be compatible with hydrogel support^{23–26}.

In this work, we demonstrate a lipid bilayer system compatible with high speed fluid exchange. We created a lipid bilayer through contact of a lipid monolayer formed at an oil/aqueous interface to a lipid monolayer formed at an oil/hydrogel interface. This contact area was masked with an aperture cut from a plastic film to help stabilize bilayer area during flow of the aqueous solution¹¹. We found that the hydrogel allowed the bilayer to tolerate flow of the aqueous solution at flow speeds up to 2.1 m/s without rupture. With these flow-stabilized bilayers, we measured the conductance of gramicidin-A channels during flow of solutions with different conductivity to precisely determine the timescale over which the solution is completely changed. Finally, we demonstrated a potential application of this device for ion channel drug potency measurements by measuring the conductance modulation of TRPM8 ion channels following rapid exchange of several solutions containing increasing drug concentrations, obtaining data for drug IC_{50} and EC_{50} values in < 4 minutes. The platform's simplicity, combined



with its compatibility with automation and parallelization^{27,28}, indicate its potential as a tool for ion channel studies and screening applications.

Results

In our recent work developing automatable, parallelizable droplet bilayer platforms^{5,28}, an aqueous droplet attached to a movable electrode composed the upper aqueous solution of the lipid membrane environment. In this work, this droplet was replaced with an agarose hydrogel droplet protruding from a pipette tip. Fabrication of these agarose droplets was simple and compatible with high throughput parallel fluid handling hardware. Once made, the hydrogels could be stored in buffer at 4 °C for weeks with no measurable difference in results. To investigate the effects of solution flow on the hydrogel-stabilized droplet bilayer membrane, we measured bilayer electrical resistance as the flow rate of the adjacent solution was increased. The solution was continuously flowed through the lower channel of the chip while the flow rate was increased every 2 seconds until the syringe pump reached its maximum drivable flow rate or until bilayer failure, indicated by a sudden, large decrease in measured resistance. Gel-supported bilayers measured in chips with a 4 mm lower channel width showed no change in resistance during flow for all pump flow rates, up to the pump's maximum, 69.5 mL/min. For the 4 mm wide lower channel, this flow rate corresponds to a flow speed in the lower channel of 0.32 m/s. To measure the effects of greater flow speeds, we produced chips with smaller lower channel widths (2 mm, 1 mm, and 0.5 mm) so that a given flow rate resulted in increased flow speeds through the lower channel. Even with these smaller channels, we were able to perfuse solution at the maximum drivable flow rate in the 2 mm and 1 mm width lower channels with no bilayer rupture, corresponding to 0.69 m/s and 1.37 m/s flow speeds. We could only observe failure of the gel-supported DIBs with a 500 μm width lower chamber at flow speeds greater than 2.1 m/s; failure was indicated by an immediate, huge reduction in electrical resistance. At high flow speeds (> 0.2 m/s) the measured electrical current in response to applied potential began to decrease with increasing flow speed, possibly due to increasing streaming potential. As a result, for the remaining measurements, the flow speed was limited to 0.1 m/s, where this effect was not observed.

Having demonstrated the stability of the gel supported droplet bilayers over a wide range of flow speeds, we investigated ion channel measurement during solution exchange using gramicidin-A (gA) as a model ion channel. We prepared agarose gel electrodes with 1 M KCl buffer and used them to make DPhPC bilayers with 3 fg/mL gA in chips with a 1 mm wide lower channel. Following bilayer formation, 100 mV was applied and steady gA currents were measured with an

average current of approximately 180 pA and fluctuations of ~ 40 pA, due to the aggregate random binding and unbinding of many conducting gA dimers²⁹. Close examination of the measured currents showed single channel steps of 2.37 ± 0.28 pA ($N = 40$) (Supplementary Information). Flow of 1 M KCl buffer through the lower channel at 5 mL/min (0.1 m/s flow speed) affected neither the magnitude of measured current nor the magnitude of the aggregated dimer current fluctuations. The observed average currents and fluctuation size also remained consistent when the flow was stopped and restarted with the syringe pump.

In another experiment exploring rapid exchange of different solutions, a solenoid valve was triggered to switch the perfused solutions between 100 mM KCl, 900 mM TEA-Cl and 1 M KCl while applying -80 mV and measuring the resultant gA current (Figure 2). The 900 mM TEA-Cl maintained the osmotic balance and chloride concentration across the bilayer while replacing gA-conductive K^+ ions with non-conductive TEA³⁰, producing a large difference in concentration of conductive K^+ ions across the bilayer after it was perfused. The solution was exchanged three times, producing four separate intervals where the measured current alternated between two distinct levels. -142 ± 5.0 pA and -9 ± 1.2 pA, measured with 1 M KCl and 100 mM KCl in the lower solutions, respectively, each averaged over the two seconds preceding the actuation of the solenoid valve. Control experiments, in which the same solutions were switched during measurement of a gel-supported bilayer containing no ion channels, showed an unchanging small measured current (< 5 pA) for all solutions over the course of the entire experiment. The difference in gA conductance in the two exchanged solutions was also seen at the single channel level. After filtering the data with a 160 Hz low pass 8-Pole Bessel filter and a 60 Hz notch filter, 1.85 ± 0.25 pA ($N = 38$) steps could be identified during measurement in the 1 M KCl solution, while 0.38 ± 0.11 pA ($N = 26$) steps were identified from the currents measured in 1 M KCl/100 mM KCl - 900 mM TEA-Cl (-80 mV potential applied throughout) (Supplementary Information).

The measured current shown in Figure 2 exhibited a consistent, approximately 750 ms lag between the triggering of the valve and the start of the change in measured current. This lag corresponds to the time required to pump the dead volume of solution in the tubing between the solenoid valve and the chamber; the dead volume is approximately 65 μL , which would take 780 ms to transfer at a flow rate of 5 mL/min, matching the observed time well. Following this initial time lag, the time required for the current to reach 90% of its steady state value from the start of its change was approximately 2.7 seconds.

We also simulated the exchange of varying ionic strength solutions through the lower chamber using COMSOL. The model geometry

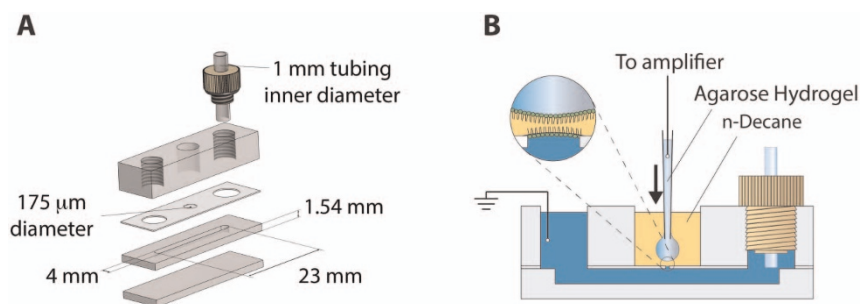


Figure 1 | Chip schematic and use. (A) Exploded view. The chip consists of four acrylic pieces: one top piece and two bottom pieces sandwich a thin middle partition containing a 175 μm diameter center aperture. The two upper holes are connected through the partition to a single channel in the lower acrylic piece and are accessible from the top. (B) Cross-sectional diagram of assembled chip in use. The lower channel is filled with liposome solution and n-decane is added to the center well. The gel-tipped electrode is dipped in liposome solution and lowered into n-decane. Following lipid monolayer formation, a lipid bilayer is formed upon contact of the gel tip to the lower aqueous solution, bounded by the partition. Transmembrane currents are recorded by an amplifier connected to the gel-tipped electrode and counter-electrode in the outer well. Connection of the lower channel fluidic inlet to a syringe pump allows exchange of the lower aqueous solution.

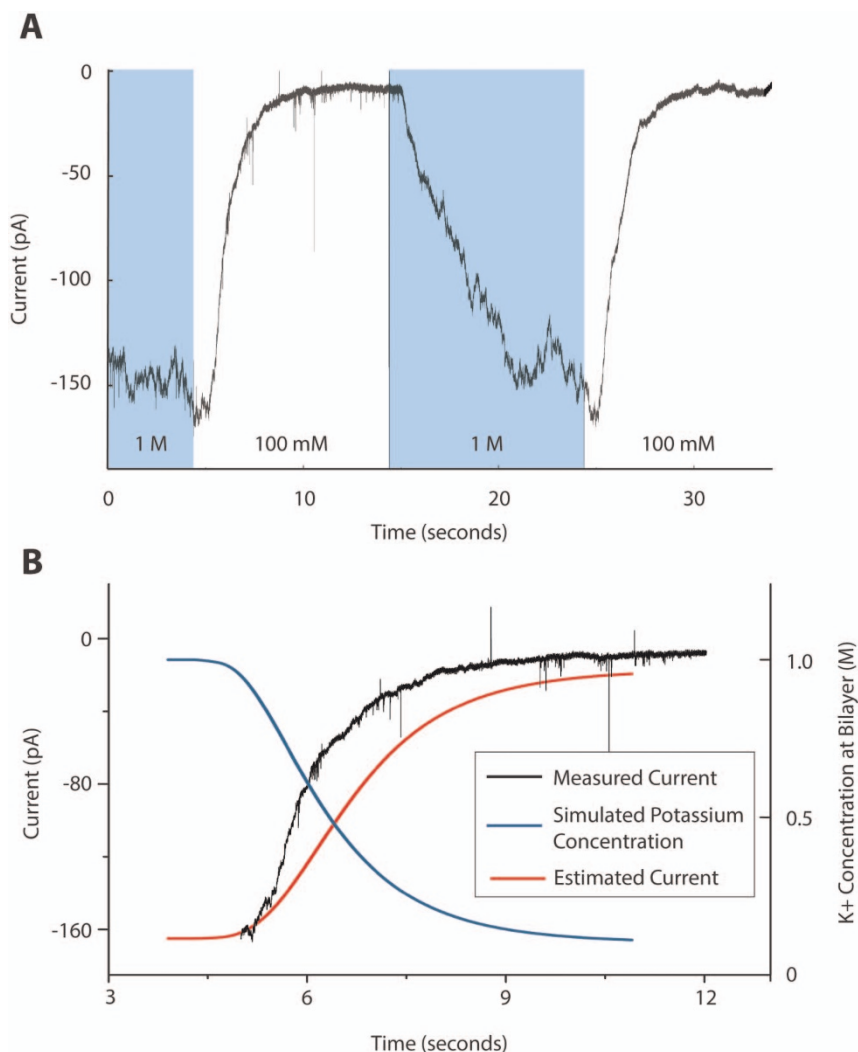


Figure 2 | (A) Unfiltered measurement of gramicidin-A conductance during repeated exchange of two different solutions. Buffered solutions containing 1 M KCl (10 mM HEPES, pH 7.2) and 100 mM KCl, 900 mM TEA-Cl (10 mM HEPES, pH 7.2) were alternately flowed through the measurement chamber during application of -80 mV transmembrane potential to a gel-supported bilayer containing gramicidin-A. The times corresponding to activation of a solenoid valve that switched between the two solutions are indicated by the shaded areas; three transitions are shown. (B) A COMSOL model simulated the K^+ concentration during exchange of the 1 M solution for the 100 mM solution (blue curve). Based on this simulated concentration and the assumption that the number of conducting gA channels remained constant, the gramicidin current was estimated using the GHK equation (red curve, see text). Measured current data from (A) is overlaid (black).

was designed to match the geometry of the chip without tubing. The laminar flow physics module was used to calculate flow through the system, using a flow velocity inlet condition and a zero pressure outlet condition. All other boundaries were given no-slip conditions. Particle tracing was calculated by the transport of diluted species physics module, defining convection of particles by the steady-state solution of the laminar flow calculation, and calculating diffusion based on a diffusion constant of 1.9×10^{-9} m²/sec³¹. Initial particle concentration was defined to be 10^{-5} mol/m³ (1 M concentration) for the entire geometry except for the inlet boundary, which was given a particle concentration of 10^{-6} mol/m³ (0.1 M), to match the conditions of the experiment shown in Figure 2a. Figure 2b shows the simulated K^+ concentration as a function of time for 7 seconds following addition of the exchanged solution at 18.4 μ s time steps.

Having demonstrated the ability of our bilayer apparatus to support high speed flow and solution exchange during ion channel measurement, we explored application of this system to rapid measurement of the potency of ion channel targeting drugs. We selected TRPM8, a mammalian ion channel responsible for cold sensing and associated with prostate and colon cancers^{32–35}, for these experiments

based on our previous work measuring its drug-modulated conductance in droplet bilayers⁴. In that previous work, TRPM8 currents were measured during the stepwise addition of menthol, an agonist compound, or 2-APB, an antagonist; these experiments required 50 to 80 minutes to complete. The length of these experiments was due in part to the sensitivity of the droplet bilayers to perturbation of surrounding solution, which necessitated extremely slow solution perfusion.

We made gel supported droplet bilayers using 200 nm diameter 3:1 POPC:POPE liposomes containing TRPM8 in buffer MB (described in Materials and Methods) containing 2.5 μ M PIP₂. While 100 mV was applied, the transmembrane current was recorded for one minute. A syringe pump loaded with a syringe containing MB and a low concentration of drug was connected to the fluid inlet and activated to introduce the solution at 0.1 m/s flow speed (20 mL/min with the 4 mm-wide channel) for 10 seconds after which it was stopped. The conductance was measured for 30 seconds; during this time, the syringe in the syringe pump was exchanged with a syringe containing a higher concentration of the drug and the process was repeated.



Experiments measuring TRPM8 currents in the presence of varying concentrations of menthol and 2-APB were performed three times each on separate bilayers (Figure 3). EC_{50} and IC_{50} values were determined by fitting the measured current data as a function of drug concentration to the Hill equation using Origin 8.5 software (OriginLab). The EC_{50} values for menthol found through these experiments were 60.9 μM , 45.4 μM , and 70.7 μM , similar to literature values of 53 to 101 μM ^{36–38}. The IC_{50} values found for 2-APB were 1.66 μM , 2.69 μM , and 3.31 μM , with literature values of 1.5 to 12 μM ^{4,39,40}. The time required to complete each set of measurements was related to the number of different concentrations measured, with four concentrations requiring 198–241 sec and eight concentrations 432 sec.

Discussion

The presence of the hydrogel on one side of the bilayer greatly increased its tolerance to solution flow, with failure only occurring at flow speeds > 2.1 m/s, much greater than the maximum flow speed seen in our previous work (2.5×10^{-4} m/s) using a highly similar system without a hydrogel¹¹. This speed is also greater than other recent reports measuring solution perfusion of droplet bilayers in microfluidic devices^{10,12}.

We hypothesize that the tolerance of the hydrogel supported membrane to increased flow speeds is a result of the increased tolerance of hydrogel supported membranes to transmembrane pressure differences, which we showed previously⁹. The hydrogel opposes deformation of the bilayer and separation from its supporting aperture. This hypothesis is consistent with the low flow rates observed in our and others' previous reported work^{10,11}. In these reports, solution exchange was driven with a syringe pump where the fluidic outlet was exposed to atmosphere. In such an apparatus, assuming a bilayer chamber with symmetric inlet and outlet fluidic connections, the hydrostatic pressure at the bilayer would be half of the inlet pressure. This inlet pressure would increase proportionally

to the flow rate, according to Poiseuille's Law. In these systems, the pressure on the other side of the bilayer is fixed because that side of the bilayer is open to atmosphere. Therefore the transmembrane pressure would also increase proportionally to the flow rate. This hypothesis also explains the higher flow rates of bilayer solution exchange in the work of Tsuji et al. through the use of a push-pull syringe pump¹². The push-pull mechanism of the pump imposes a positive pressure on the inlet of the channel and a matching negative pressure on the outlet of the channel, resulting in a fluid pressure close to atmospheric pressure near the bilayer and therefore a greatly reduced pressure gradient across the bilayer. Therefore, higher flow rates can be tolerated before bilayer rupture. Our approach offers two advantages: first, we were able to obtain higher flow rates. Second, a push-only solution exchange system is much more amenable to parallelization and automation such as with multi-channel robotic pipette heads.

Although the rate of fluid flow through the measurement chamber may be easily controlled and determined by the syringe pump, ascertaining the exact time for which the measurement solution is fully exchanged is complicated by the static fluid boundary layer at the chamber walls and the exact position of the bilayer relative to the flowing solution. Our measurements of gA during flow were intended to empirically monitor the progress of solution exchange by continuously measuring gA current as the measurement solution was switched between 1 M and 100 mM concentrations of the only conductive ion, potassium.

Two main effects were expected when switching between the lower solution from 1 M to 100 mM: 1) establishment of a Nernst potential from 0 mV to $V_N = -\frac{k_B T}{e} \ln \frac{a_{\text{gel}}}{a_{\text{lower}}} = -54$ mV, where a_{gel} is the 1 M K^+ activity⁴¹ (0.6 M) and a_{lower} is the 100 mM K^+ activity⁴¹ (0.074 M) and 2) decreased K^+ conductivity in the lower solution. Since we constantly applied -80 mV in these measurements, we expected both of these effects to result in a lower measured current.

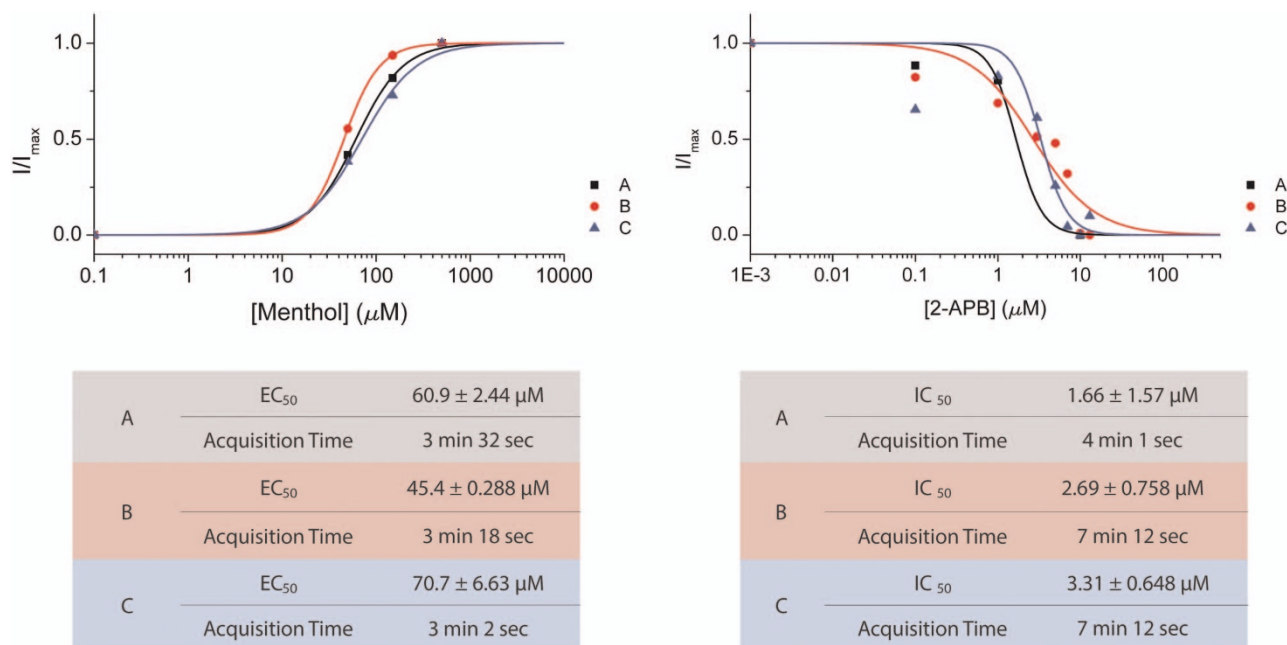


Figure 3 | TRPM8 activation and inhibition by menthol and 2-APB, respectively. (Left) In three separate experiments (A), (B), (C), menthol was perfused into the chip in increasing concentrations (0, 50, 150, 500 μM) and the current was measured for 30 seconds while applying 100 mV. These currents were averaged and normalized to the current measured at 500 μM menthol. EC_{50} values were obtained from fits of the data to the Hill equation. (Right) In three experiments, 2-APB was perfused into the chip in increasing concentrations in solutions also containing 500 μM menthol. Currents were measured similarly to the previous menthol experiments (Left). In one experiment (A), the 2-APB concentrations measured were 0, 0.1, 10, 13 μM . In two experiments (B), (C) the concentrations were 0, 0.1, 1, 3, 5, 7, 10, 13 μM . IC_{50} values were obtained from fits of the data to the Hill equation. Acquisition times represent the total time from initiation to conclusion of all measurements.



We can quantitatively estimate the expected current level by using the Goldman-Hodgkin-Katz current equation⁴² for potassium:

$$I_K = \frac{e^2 1000 N_A P_K}{k_B T} V \left[\frac{a_{\text{lower}} e^{-\frac{eV}{k_B T}} - a_{\text{gel}}}{e^{-\frac{eV}{k_B T}} - 1} \right] \quad (1)$$

$$= G_K(a_{\text{lower}}) V \left[\frac{e^{-\frac{eV}{k_B T}} - \frac{a_{\text{gel}}}{a_{\text{lower}}}}{e^{-\frac{eV}{k_B T}} - 1} \right]$$

where V is the potential applied between the tip and lower channel, k_B is 1.38×10^{-23} J/K, T is the temperature, e is 1.602×10^{-19} C, N_A is 6.02×10^{23} , and P_K is the permeability of the bilayer to potassium. After factoring a_{lower} from the bracketed expression, we define $G_K(a_{\text{lower}})$ as $G_K = \frac{e^2 1000 N_A P_K}{k_B T} a_{\text{lower}}$. Therefore, when the K concentrations in the gel and lower channel are both 1 M, $I_{K,1M} = G_K(a_{1M})V$. The single channel gA current steps measured with 1 M KCl present on both sides of the bilayer were 1.85 pA, a conductance of 23 pS at -80 mV, consistent with ~ 21 pS of previous work⁴³. Upon exchanging the lower solution to 100 mM KCl, 0.38 pA steps were identified. With the K concentration in the gel and lower solutions of 1 M and 0.1 M, respectively, Eq. 1 becomes $I_K = G_K(a_{\text{lower}}) * V * 0.66$, and the gA conductance we obtain for these steps is 7.2 pS, comparable to ~ 9 pS measured at 100 mV in 0.1 M KCl by Busath et al. in DPhPC bilayers⁴³.

In Figure 2, the current measured before the actuation of the solenoid at $t = 4.5$ seconds was -165 pA, corresponding to a conductance G_K of 2063 pS, approximately 90 channels. The current is stabilized following the solution exchange at approximately 9 pA, a conductance of 170 pS from Equation 1. From our single channel conductance measurement of 0.38 pA, 9 pA is approximately 24 channels, a significant reduction from the 90 estimated prior to the solution exchange. A reduction in the number of channels is consistent with previous reports of a reduction in gA's dimer equilibrium constant with a reduction in electrolyte concentration⁴⁴.

The time course of the simulated concentration can be related to the measured current through application of the simulated data to Equation 1. The ionic activity was found from the concentration using the data from Hamer and Wu⁴¹, and the gA single channel conductance in DPhPC for different KCl concentrations was found from Busath et al.⁴³. The data from Busath et al. was measured in symmetric solutions and without TEA-Cl, and so it may not be fully applicable here. The activity and gA conductance was input into Equation 1 for calculated estimates of the gA current as a function of time (Figure 2b). The measured current appears to decrease faster and plateau at a smaller magnitude than the predicted current. As the predicted current assumes that the number of conducting channels in the bilayer is constant, this could be explained by our observation of the number of conducting channels decreasing during the solution exchange. The time for the simulated concentration to fall 90% from 1 M to 0.1 M is 3.7 seconds, the same time required for the calculated current to rise 90% from -165 pA to -19.6 pA. The measured current required only 2.5 seconds to rise 90% from -165 pA to -7.3 pA. The faster than predicted decrease in current is also consistent with the decreased number of conducting channels measured in the lower concentration.

Tsuji and coworkers recently reported solution exchange surrounding a bilayer using a push-pull syringe pump and measured the exchange time through fluorescence measurement as the fluorophore was removed from the observed solution¹². Their simulations of the non-laminar flow showed that the solution adjacent to the bilayer flowed at approximately 1/5 of the pumped rate, indicating the effects of the boundary layer to effectively slow the flow near the bilayer. This slowed flow resulted in a time for the fluorescence decrease to 1% of its initial value of 16.5 seconds.

For repeated ion channel measurement in a series of exchanged solutions, the total time required will be the sum of the time for solution exchange and the time for the measurements themselves. In the series of TRPM8 measurements described here, the solution flow speed was 0.1 m/s which resulted in approximately 4.5 sec for complete solution exchange (Figure 2). To ensure that the solutions were entirely exchanged, we flowed the solutions for 10 sec before deactivating the pump. The following 30 second measurement time was also conservatively chosen to minimize statistical uncertainty in determination of the average current. Taken together and including the time required for fluid handling, the total measurement time per drug concentration was at least 50 seconds, requiring approximately 200 and 400 seconds for four and eight measured concentrations respectively. This is a good improvement over previous measurements of concentration-dependent drug interactions with ion channels in lipid bilayers⁴⁻⁷, in which slow rates of exchange of measurement solution were primary factors contributing to assay times greater than one hour.

In conclusion, we have demonstrated that hydrogel-supported lipid bilayers are sufficiently robust to withstand the exchange of adjacent solution at high flow rates (> 2 m/s) without bilayer rupture. Rapid exchange of the measurement solution enables increased measurement efficiency and throughput. Our bilayer chip and measurement apparatus allowed electrical measurement of the bilayer and ion channels during flow. Using this apparatus, we were able to measure the concentration-dependent inhibition of the conductance of the ion channel TRPM8, obtaining IC_{50} and EC_{50} values in minutes, versus previously reported times on the order of an hour.

As with our previous work, the upper and lower halves of the bilayer are accessible from the top of the chip for fluid addition and bilayer formation and measurement^{4,5}. The gel-tipped electrodes integrate bilayer formation and measurement and require only simple vertical translation to begin the assay. This step, and the addition of the solutions to the chip, can be easily automated²⁸ and parallelized²⁷ with the construction of repeated arrays of the basic chip design shown in Figure 1. The gel-tipped electrodes can be mass-prepared in advance of the measurement and stored until use. These advantages and the short assay time give this platform potential for high throughput measurement and screening.

Methods

Unless otherwise noted, all reagents and chemicals were purchased from Sigma Aldrich.

Bilayer chip. The bilayer chip design (Figure 1A) was adapted from previous work^{5,28}. The chip was laser cut from acrylic sheets (McMaster Carr, Techplast). The chip top was $1/4''$ thick with three collinear holes 5 mm in diameter. The outer holes were tapped with 10–32 size threads to accommodate fluidic connections. The bottom of the chip consisted of a 23 mm long channel ranging from 0.5 to 4 mm in width (depending on the experiment) formed from two $1/16''$ thick acrylic sheets. Between the chip top and bottom was a 250 μ m thick acrylic sheet containing three collinear holes with center positions matching those of the chip top. Two peripheral holes had 5 mm diameter matching the inlet/outlet ports of the chip top and a 175 μ m diameter hole aligned with the central hole of the chip top. The 175 μ m diameter hole was cut at the center of a 2.5 mm diameter region in which the acrylic was thinned using the laser to 100 ± 2 μ m thickness, as measured by a digital micrometer (Mitutoyo). Once assembled, the lower channel is accessible through the peripheral holes in the chip top and connects to the upper part of the center well through only the 175 μ m diameter hole. After assembly, the chip was glued using Weld-On Type 4 (SCI Grip).

Bilayer formation. 200 nm diameter liposomes, composed of 250 μ g/mL diphytanoylphosphatidylcholine (DPhPC) or 250 μ g/mL of 3 : 1 (w : w) 1-palmitoyl-2-oleoyl-sn-glycero-3-phosphocholine (POPC) and 1-palmitoyl-2-oleoyl-sn-glycero-3-phosphoethanolamine (POPE) (Avanti Polar Lipids), were prepared by extrusion through a 200 nm filter in measurement buffer MB (150 mM KCl, 0.2 mM $MgCl_2$ (10 mM HEPES, pH 7.2) or 1 M KCl (10 mM HEPES, pH 7.2)). The chip was prepared for use by filling the lower chamber through the peripheral wells with 200 μ L of the liposome solution followed by addition of 80 μ L of n-decane to the upper central well (Figure 1B). 1.35 μ L of the liposome solution was deposited onto an agarose gel bead (described below) and the gel bead was lowered into the central well until it was completely submerged in n-decane (Figure 1B). After a waiting period



of 5 minutes to allow lipid monolayers to form, the gel bead was lowered to contact the 175 μm diameter aperture where the bilayer formed once the monolayers contacted.

Sessile agarose droplet. A 1% (w/v) solution of low melting point agarose (Invitrogen) was prepared in MB, except during experiments varying ionic strength, when it was prepared in 1 M KCl (10 mM HEPES, pH 7.2). The solution was warmed to 50°C and approximately 100 μL of it was drawn into a 200 μL gel-loading pipette tip (VWR). The solution was slowly dispensed out of the pipette tip to form a ~ 3 μL sessile droplet at the end of the tip, which was cooled to the gel state. The pipette tip was then backfilled with MB or 1 M KCl and stored with the agarose sessile droplet immersed in the same solution at 4°C. Formation of gel tipped electrodes in this way was easy and rapid, and they were storable for extended periods of time at 4°C.

Electrophysiological measurement. Ag/AgCl electrodes were inserted into the top of the pipette gel tip and the outlet port of the bilayer chip and connected to an Axopatch 200B amplifier (Axon Instruments), which applied a 1 kHz Bessel filter to the amplified currents. The resulting signals were digitized at 10 kHz (Digidata 1440A, Axon Instruments) and further filtered and analyzed with Clampfit 10 software (Axon Instruments).

Gramicidin-A channels were diluted to 3 $\mu\text{g}/\text{mL}$ in a solution of DPhPC liposomes in 1 M KCl (10 mM HEPES, pH 7.2) and used for bilayer formation, as previously described. Rat TRPM8 ion channels were purified and reconstituted into 3:1 POPC:POPE liposomes at a 1:1,000 protein:lipid ratio (w:w), as previously reported^{44,45}. 10 $\mu\text{g}/\text{mL}$ proteoliposome stock solutions were diluted to 1 $\mu\text{g}/\text{mL}$ prior to measurement in MB and 2.5 μM phosphatidylinositol-4,5-bisphosphate (PI(4,5)P₂, Avanti Polar Lipids), a compound required for TRPM8 activation⁴⁵. All experiments were conducted at room temperature, approximately 21°C.

Solution exchange. 30 mL plastic syringes (Becton-Dickinson) were connected to the inlet hole of the bilayer chip by 1 mm inner diameter Teflon tubing (Sigma-Aldrich) and 10–32 size flangeless fittings (Sigma-Aldrich). The syringes were driven by a single syringe pump (KDS Legato 200, KD Scientific), controlled through Windows HyperTerminal command prompts to drive solution at variable rates through the bilayer chip's lower channel (Figure 1B). For experiments in which perfusion of two solutions was alternated, a system of four two-way solenoid valves directed and alternated flow from two syringes such that flow from one syringe went to the bilayer chip, and flow from the other syringe went into a waste container. In experiments in which more than two solutions were perfused into the chip, a solenoid valve was switched to direct flow from an external line to the syringe. The syringe was then filled with the appropriate perfusion solution, and the valve was switched back to direct flow toward the chip. Solenoid valve actuation was controlled was LabVIEW 9.2.1 software (National Instruments).

In experiments in which perfusion speed limits were explored, the solution used was MB. In experiments in which the composition of the lower aqueous solution was changed (Fig. 2), 1 M KCl (10 mM HEPES, pH 7.2) and 100 mM KCl, 900 mM Tetraethylammonium Chloride (TEA-Cl) (10 mM HEPES, pH 7.2) buffer were used. During measurements of TRPM8 (Fig. 3), MB solutions containing varying concentrations of Menthol or 2-Aminoethoxydiphenyl Borate (2-APB) were used.

Ion convection and diffusion modeling. COMSOL Multiphysics 4.2 a (COMSOL, Stockholm, Sweden) was used to model the solution flow through the lower chamber during exchange of 1 M KCl solution for 0.1 M KCl. The Laminar Flow physics module was used to calculate flow through the system, using a flow velocity inlet condition and a zero pressure outlet condition. All other boundaries were given no-slip constraints. Particle tracing was calculated by the Transport of Diluted Species physics module, defining convection of particles by the steady-state solution of the laminar flow calculation and calculating diffusion based on a diffusion constant of 1.9×10^{-9} m^2/sec^31 . Initial particle concentration was defined to be 1 M for the entire geometry except for the inlet boundary, which was given a particle concentration of 1 M to match the transitions between shaded and unshaded regions in Figure 2.

1. Schindler, H. & Quast, U. Functional acetylcholine receptor from Torpedo marmorata in planar membranes. *Proc. Natl. Acad. Sci. USA* **77**, 3052–3056 (1980).
2. *Ion channel reconstitution*, Miller, C. (ed.) (Plenum Press, 1986).
3. Bayley, H. & Cremer, P. S. Stochastic sensors inspired by biology. *Nature* **413**, 226–230 (2001).
4. El-Arabi, A. M., Salazar, C. S. & Schmidt, J. J. Ion channel drug potency assay with an artificial bilayer chip. *Lab Chip* **12**, 2409–2413, doi:10.1039/c2lc40087a (2012).
5. Portonovo, S. A., Salazar, C. S. & Schmidt, J. J. hERG drug response measured in droplet bilayers. *Biomed. Microdev.* doi:10.1007/s10544-012-9725-9 (2012).
6. Syeda, R., Holden, M. A., Hwang, W. L. & Bayley, H. Screening blockers against a potassium channel with a droplet interface bilayer array. *J. Am. Chem. Soc.* **130**, 15543–15548 (2008).
7. Tao, X. & MacKinnon, R. Functional analysis of Kv1. 2 and paddle chimera Kv channels in planar lipid bilayers. *J. Mol. Biol.* **382**, 24–33 (2008).
8. Schneider, G. F. & Dekker, C. DNA sequencing with nanopores. *Nat. Biotechnol.* **30**, 326–328 (2012).
9. Malmstadt, N., Jeon, T. J. & Schmidt, J. J. Long-lived Planar Lipid Bilayer Membranes Anchored to an In Situ Polymerized Hydrogel. *Adv. Mater.* **20**, 84–89 (2008).

10. Shao, C., Sun, B., Colombini, M. & DeVoe, D. L. Rapid Microfluidic Perfusion Enabling Kinetic Studies of Lipid Ion Channels in a Bilayer Lipid Membrane Chip. *Ann. Biomed. Eng.* **39**, 2242–2251 (2011).
11. Portonovo, S. A. & Schmidt, J. Masking apertures enabling automation and solution exchange in sessile droplet lipid bilayers. *Biomed. Microdev.* **14**, 187–191 (2012).
12. Tsuji, Y. *et al.* Droplet based lipid bilayer system integrated with microfluidic channels for solution exchange. *Lab Chip* (2013).
13. Egorova, E. M., Chernomordik, L. V., Abidor, I. G. & Chizmadzhev, Y. A. Liposome fusion with planar lipid membranes. *Biofizika* **26**, 145–147 (1981).
14. Gutknecht, J. Inorganic mercury (Hg 2+) transport through lipid bilayer membranes. *J. Membr. Biol.* **61**, 61–66 (1981).
15. Schadt, M. & Haeussler, G. Permeability of lipid bilayer membranes to biogenic amines and cations: changes induced by ionophores and correlations with biological activities. *J. Membr. Biol.* **18**, 277–294 (1974).
16. Pintschovius, J. & Fendler, K. Charge Translocation by the Na⁺/K⁺-ATPase Investigated on Solid Supported Membranes: Rapid Solution Exchange with a New Technique. *Biophys J* **76**, 814–826 (1999).
17. Jeon, T.-J., Malmstadt, N. & Schmidt, J. J. Hydrogel-Encapsulated Lipid Membranes. *J. Am. Chem. Soc.* **128**, 42–43 (2006).
18. Kang, X. F., Cheley, S., Rice-Ficht, A. C. & Bayley, H. A storable encapsulated bilayer chip containing a single protein nanopore. *J. Am. Chem. Soc.* **129**, 4701–4705 (2007).
19. Shim, J. W. & Gu, L. Q. Stochastic sensing on a modular chip containing a single-ion channel. *Anal Chem* **79**, 2207–2213 (2007).
20. Funakoshi, K., Suzuki, H. & Takeuchi, S. Lipid bilayer formation by contacting monolayers in a microfluidic device for membrane protein analysis. *Anal Chem* **78**, 8169–8174, doi:10.1021/ac0613479 (2006).
21. Zagnoni, M., Sandison, M. E., Marius, P. & Morgan, H. Bilayer lipid membranes from falling droplets. *Anal. Bioanal. Chem.* **393**, 1601–1605 doi:10.1007/s00216-008-2588-5 (2009).
22. Bayley, H. *et al.* Droplet interface bilayers. *Mol. Biosyst.* **4**, 1191–1208 (2008).
23. Ide, T., Kobayashi, T. & Hirano, M. Lipid bilayers at the gel interface for single ion channel recordings. *Anal Chem* **80**, 7792–7795 (2008).
24. Sarles, S. A., Stiltner, L. J., Williams, C. B. & Leo, D. J. Bilayer formation between lipid-encased hydrogels contained in solid substrates. *ACS Appl. Mater. Interfaces* **2**, 3654–3663 (2010).
25. Thompson, J. R., Heron, A. J., Santos, Y. & Wallace, M. I. Enhanced stability and fluidity in droplet on hydrogel bilayers for measuring membrane protein diffusion. *Nano Lett.* **7**, 3875–3878 (2007).
26. Lu, X., Leitmannova Ottova, A. & Tien, H. T. Biophysical aspects of agar-gel supported bilayer lipid membranes: a new method for forming and studying planar bilayer lipid membranes. *Bioelectrochem. Bioenerg.* **39**, 285–289 (1996).
27. Poulos, J. L. *et al.* Ion channel and toxin measurement using a high throughput lipid membrane platform. *Biosens. Bioelectron.* **24**, 1806–1810 (2009).
28. Poulos, J., Portonovo, S., Bang, H. & Schmidt, J. Automatable lipid bilayer formation and ion channel measurement using sessile droplets. *J. Phys.: Condens. Matter* **22**, 454105 (2010).
29. Bamberg, E. & Läuger, P. Channel formation kinetics of gramicidin A in lipid bilayer membranes. *J. Membr. Biol.* **11**, 177–194 (1973).
30. Andersen, O. Ion movement through gramicidin A channels. Single-channel measurements at very high potentials. *Biophys. J.* **41**, 119–133 (1983).
31. Mamonov, A. B., Kurnikova, M. G. & Coalson, R. D. Diffusion constant of K⁺ inside Gramicidin A: A comparative study of four computational methods. *Biophys. Chem.* **124**, 268–278 (2006).
32. McKemy, D. D., Neuhauser, W. M. & Julius, D. Identification of a cold receptor reveals a general role for TRP channels in thermosensation. *Nature* **416**, 52–58 (2002).
33. Peier, A. M. *et al.* A TRP channel that senses cold stimuli and menthol. *Cell* **108**, 705–715 (2002).
34. Tsavalas, L., Shapero, M. H., Morkowski, S. & Laus, R. Trp-p8, a novel prostate-specific gene, is up-regulated in prostate cancer and other malignancies and shares high homology with transient receptor potential calcium channel proteins. *Cancer Res.* **61**, 3760–3769 (2001).
35. Zhang, L. & Barritt, G. J. TRPM8 in prostate cancer cells: a potential diagnostic and prognostic marker with a secretory function? *Endocr.-Relat. Cancer* **13**, 27–38 (2006).
36. Andersson, D. A., Chase, H. W. N. & Bevan, S. TRPM8 activation by menthol, icilin, and cold is differentially modulated by intracellular pH. *J. Neurosci.* **24**, 5364–5369 (2004).
37. Tsuruda, P. R., Julius, D. & Minor, D. L. Coiled Coils Direct Assembly of a Cold-Activated TRP Channel. *Neuron* **51**, 201–212 (2006).
38. McKemy, D. D. Therapeutic potential of TRPM8 modulators. *Open Drug Discov. J* **2**, 81–88 (2010).
39. Hu, H. Z. *et al.* 2-aminoethoxydiphenyl borate is a common activator of TRPV1, TRPV2, and TRPV3. *J. Biol. Chem.* **279**, 35741–35748 (2004).
40. ChanTest, Stably Transfected Cell Line - Product Data Sheet hTRPM8-CHO, http://www.chantest.com/media/cms/pdf/data_CT6193.pdf, Date of Access April 1 2013.
41. Hamer, W. J. & Wu, Y.-C. Osmotic coefficients and mean activity coefficients of uni-univalent electrolytes in water at 25 C. *J. Phys. Chem. Ref. Data* **1**, 1047–1099 (1972).



42. Hille, B. *Ion Channels of Excitable Membranes*. (Sinauer Associates, 2001).
43. Busath, D. D. *et al.* Noncontact Dipole Effects on Channel Permeation. I. Experiments with (5F-Indole)Trp13 Gramicidin A Channels. *Biophys. J.* **75**, 2830–2844 (1998).
44. Kolb, H. A. & Bamberg, E. Influence of membrane thickness and ion concentration on the properties of the gramicidin A channel Autocorrelation, spectral power density, relaxation and single-channel studies. *BBA-Biomembranes* **464**, 127–141 (1977).
45. Zakharian, E., Cao, C. & Rohacs, T. Gating of transient receptor potential melastatin 8 (TRPM8) channels activated by cold and chemical agonists in planar lipid bilayers. *J. Neurosci.* **30**, 12526–12534 (2010).

Acknowledgments

We thank Dino Di Carlo, Takasi Nisisako, and Ahmad El-Arabi for consultation and Quincy Chen for assistance with chip fabrication.

Author contributions

J.S. conceived the study design and analyzed data. S.A., A.P., C.S. contributed to experiment design, performed experiments, and analyzed data. S.A. and A.P. contributed to device

concept and fabrication. S.A., C.S. and J.S. drafted the paper. All of the authors discussed the results and edited the manuscript.

Additional information

Supplementary information accompanies this paper at <http://www.nature.com/scientificreports>

Competing financial interests: The authors declare no competing financial interests.

How to cite this article: Acharya, S.A., Portman, A., Salazar, C.S. & Schmidt, J.J. Hydrogel-Stabilized Droplet Bilayers for High Speed Solution Exchange. *Sci. Rep.* **3**, 3139; DOI:10.1038/srep03139 (2013).



This work is licensed under a Creative Commons Attribution-NonCommercial-ShareAlike 3.0 Unported license. To view a copy of this license, visit <http://creativecommons.org/licenses/by-nc-sa/3.0>